

RESEARCH ARTICLE



Safety and biocompatibility of a novel biodegradable aflibercept-drug delivery system in rhesus macaques

Brett D. Story^a, Sangwan Park^a, Karolina Roszak^a, Jaeho Shim^a, Monica Motta^a, Michelle Ferneding^a, Kayla M. Rudeen^{b,c}, Andrew Blandino^d, Monica Ardon^a, Sophie Le^a, Leandro B. C. Teixeira^e, Glenn Yiu^f, William F. Mieler^g, Sara M. Thomasy^{a,f,h} and Jennifer J. Kang-Mielerⁱ

^aDepartment of Surgical and Radiological Sciences, School of Veterinary Medicine, University of California–Davis, Davis, CA, USA; ^bDepartment of Biomedical Engineering, Illinois Institute of Technology, Chicago, IL, USA; ^cLocal Delivery Translational Sciences, AbbVie, North Chicago, IL, USA; ^dDepartment of Statistics, University of California, Davis, CA, USA; ^eDepartment of Pathobiological Sciences, School of Veterinary Medicine, University of Wisconsin–Madison, Madison, WI, USA; ^fDepartment of Ophthalmology & Vision Science, University of California, Davis, Sacramento, CA, USA; ^gDepartment of Ophthalmology and Visual Sciences, Illinois Eye and Ear Infirmary, University of Illinois, Chicago, IL, USA; ^hCalifornia National Primate Research Center, Davis, CA, USA; ⁱDepartment of Biomedical Engineering, Stevens Institute of Technology, Hoboken, NJ, USA

ABSTRACT

A clinical need exists for more effective intravitreal (IVT) drug delivery systems (DDS). This study tested the hypothesis that a novel biodegradable, injectable microsphere-hydrogel drug delivery system loaded with aflibercept (aflibercept-DDS) would exhibit long-term safety and biocompatibility in a non-human primate (NHP) model. We generated aflibercept-loaded poly (lactic-co-glycolic acid) microparticles with a modified double emulsion technique then embedded them into a biodegradable, thermo-responsive poly (ethylene glycol)-co-(L-lactic-acid) diacrylate/N-isopropylacrylamide hydrogel. Aflibercept-DDS (50 µL, 15 µg) was injected into the right eye of 23 healthy rhesus macaques. A complete ophthalmic examination, intraocular pressure (IOP), corneal pachymetry, specular microscopy, A-scan biometry, streak retinoscopy, spectral-domain optical coherence tomography (SD-OCT), fluorescein angiography (FA), and electroretinography (ERG) were performed monthly. Globes from 7 NHPs were histologically examined. Aflibercept-DDS was visualized in the vitreous up to 9 months post-IVT injection, slightly impeding funduscopy in 4 of 23 eyes; no other consistent abnormalities were appreciated during ophthalmic examination. The IOP and total retinal thickness remained normal in all animals over all timepoints. Central corneal thickness, endothelial cell density, axial globe length, and refractive error did not significantly differ from baseline. Scotopic mixed rod-cone implicit times and amplitudes along with photopic cone response implicit times and amplitudes did not significantly differ from control values. No retinal or choroidal vascular abnormalities were detected with FA and normal retinal architecture was preserved using SD-OCT. Intravitreal injection of a biodegradable aflibercept-DDS was safe and well tolerated in NHPs up to 24 months.

ARTICLE HISTORY

Received 28 June 2024
Revised 1 December 2024
Accepted 24 January 2025

KEYWORDS

aflibercept; anti-VEGF; controlled drug delivery; intravitreal injection; nonhuman primate; thermo-responsive hydrogel


Introduction

Intravitreal (IVT) injections of anti-vascular endothelial growth factor (anti-VEGF) have become a mainstay in the treatment of age related macular degeneration (AMD), undoubtedly leading to significant visual improvement in affected patients (Brown et al., 2009; Rosenfeld et al., 2006). Anti-VEGF treatments such as intravitreal injection of aflibercept are the standard of care for AMD (Heier et al., 2012). Additionally, aflibercept requires less frequent administration than ranibizumab to achieve a similar therapeutic outcome (Heier et al., 2012; Wykoff et al., 2023; Lanzetta et al., 2024). Dual inhibitors of angiopoietin-2 and VEGF-A have also become recently available (Heier et al., 2022). Although these treatments have improved management for vascular macular diseases, the burden of frequent monthly visits and patient injections

coupled with physician and health-care system related stress cannot be denied. Indeed, most patients require more than one injection, with some requiring 7–8 injections during the first year of treatment (Stahl, 2020). In nearly all patients, anti-VEGF injections must be continued over a long period of time (Chandra et al., 2020). With AMD being one of the leading causes of blindness worldwide and an estimated 22 million people affected by 2050 in the United States alone (Flaxel et al., 2020), clearly a more effective drug delivery system (DDS) for anti-VEGF is required.

Achieving target therapeutic drug concentrations to the posterior segment remains a challenge for clinicians due to ocular anatomy. The highly specialized blood-ocular barriers selectively prevent compounds from reaching the posterior segment (Leclercq et al., 2022). This is beneficial with regards to potential pathogens, but also limits many therapeutic

CONTACT Brett D. Story  bdstory@ucdavis.edu

 Supplemental data for this article can be accessed online at <https://doi.org/10.1080/10717544.2025.2460671>.

© 2025 The Author(s). Published by Informa UK Limited, trading as Taylor & Francis Group.

This is an Open Access article distributed under the terms of the Creative Commons Attribution-NonCommercial License (<http://creativecommons.org/licenses/by-nc/4.0/>), which permits unrestricted non-commercial use, distribution, and reproduction in any medium, provided the original work is properly cited. The terms on which this article has been published allow the posting of the Accepted Manuscript in a repository by the author(s) or with their consent.

drugs from reaching target concentrations. Intravitreal injection remains the most direct and efficient method for delivery of therapeutic drug concentrations to the posterior segment and it is one of the most performed procedures by retinal specialists. However, a major limitation for IVT injections of anti-VEGF agents is short drug half-life and fast clearance rate, necessitating frequent therapy (Zhu et al., 2008; Xu et al., 2013). Additionally, bolus drug administration leads to initial high peak drug concentrations following injection that plateaus and is rapidly cleared between injections promoting disease progression (El Sanharawi et al., 2010). Although the injections are often well-tolerated, sight-threatening complications include retinal detachment, endophthalmitis, and/or retinal vasculitis (Patel et al., 2022).

There remains a critical need for more effective (Luo et al., 2021; Anand et al., 2023; Nguyen et al., 2023; Jian et al., 2024) and long-lasting drug delivery systems for posterior segment disease. An ideal DDS would maintain steady-state continuous release and would be fully biodegradable. We have developed a DDS that consists of biodegradable poly lactic-co-glycolic acid (PLGA) microspheres suspended inside a thermo-responsive hydrogel (Osswald and Kang-Mieler, 2015; Osswald and Kang-Mieler, 2016). Thermo-responsive hydrogels present a unique property for drug delivery owed to the ability to change physical state rapidly and reversibly in response to temperature. At room temperature (22°C), the hydrogel is in a liquid-like form and the above transition temperature (32°C), the hydrogel collapses to solid-like form (Liu et al., 2019). The thermo-responsive hydrogel that is the basis of our DDS is easy to administer via IVT injection and undergoes a rapid transformation into a viscoelastic solid once reaching vitreal physiologic temperatures (Osswald et al., 2017). Recently, thermo-responsive hydrogels have showed promise as long-acting drug delivery systems (Nguyen et al., 2020) particularly for management of glaucoma (Nguyen et al., 2019; Luo et al., 2020). In many US Food and Drug Administration-approved therapeutic devices, PLGA has been used to deliver numerous drugs for durations ranging from weeks to months (Holmkvist et al., 2016; Osswald and Kang-Mieler, 2016; Kang-Mieler et al., 2014; Park et al., 2018). Tailored drug characteristics and sustained release profiles can be achieved by encapsulating drugs within PLGA microspheres (Osswald and Kang-Mieler, 2015) with our previous studies documenting release of bioactive VEGF from PLGA microspheres for ~200 days (Osswald and Kang-Mieler, 2015; Osswald et al., 2017). Using PLGA for a DDS is crucial for ocular delivery due to its biodegradability, particularly since multiple intraocular injections are anticipated. The PLGA microspheres achieve controlled and extended release of therapeutics, and their biodegradation products do not cause retinal cell death, glial activation, or inflammatory reactions as detailed in rabbit models (Rong et al., 2014).

Recently, we demonstrated that IVT injection of biodegradable microspheres in a non-biodegradable hydrogel aflibercept-DDS can achieve controlled, sustained release with no adverse effects for up to 6 months in the eyes of healthy rhesus macaques (Kim et al., 2020). The eyes of rhesus macaque demonstrate similar anatomy, physiology, pharmacology, and immunology to those of humans and are thus

an invaluable research model (Lin et al., 2021; 2021; Sazhnyev et al., 2023). The presence of a macula highlights the importance of NHPs as an animal model for macular disease such as AMD. To further investigate the potential usage of anti-VEGF-loaded DDS in human clinical trials an ideal DDS must first demonstrate safety of a fully biodegradable system. Thus, the purpose of this study was to evaluate the safety of bioactive encapsulated aflibercept released from a biodegradable microsphere-hydrogel DDS using a NHP model.

Materials and methods

Production of a novel biodegradable aflibercept-DDS

Aflibercept (15 µg; 40 mg/ml)-loaded PLGA 75:25 microspheres with an encapsulation efficiency of 45% were fabricated using a modified double-emulsion, solvent evaporation technique described in detail elsewhere (Liu et al., 2019; Liu et al., 2019; Liu et al., 2020). The primary aqueous phase (W1) was prepared by mixing 100 µL of an aflibercept solution (40 mg/mL) with excipients, including 12.5 mg bovine serum albumin (BSA), 10 mg polyethylene glycol 8000 (PEG-8000), and 2.5 mg sucrose. The oil phase (O) was prepared by dissolving 125 mg of 75:25 PLGA in 0.5 mL of dichloromethane (DCM) along with 4 mg of magnesium hydroxide (Mg(OH)₂) as a buffering agent. The first emulsion (W1/O) of the primary aqueous phase into the oil phase was created by vortexing. Subsequently, the first emulsion was added into 5 mL of 10% polyvinyl alcohol (PVA) to form the secondary emulsion (W1/O/W2) by vortexing and then stirred in 75 mL of 0.2% PVA for 3 hours to evaporate DCM. After solvent evaporation, microspheres were harvested by centrifugation, washed three times in deionized (DI) water, lyophilized to a dry powder, and stored at 4°C. Degradable thermo-responsive hydrogels composed of poly(ethylene glycol)-co-(L-lactic acid) diacrylate (PEG-PLLA-DA) and N-isopropylacrylamide (NIPAAm) were synthesized by free radical polymerization method described in detail elsewhere (Drapala et al., 2014). Briefly, hydrogel precursors were prepared by dissolving 2 mM PEG-PLLA-DA, 350 mM NIPAAm, 50 mM N-tert-butylacrylamide, and 13 mM ammonium persulfate in pH 7.4 1× phosphate-buffered saline (PBS). Under sterile conditions, the hydrogel precursor and initiator were filtered through a sterile 13 mm syringe filter (0.22 µm; Fisherbrand, Thermo Fisher Scientific, Waltham, MA, USA). Aflibercept-loaded microspheres were suspended in hydrogel precursor at 20 mg/ml concentration. Polymerization of the hydrogel was initiated by mixing 168 mM N,N,N',N'-tetramethylethylenediamine (pH adjusted to 7.4 with hydrochloric acid) into the hydrogel precursor; the reaction was allowed to proceed on ice for 30 minutes to form microsphere-hydrogel DDS. After polymerization, DDSs were collected, washed three times in sterile DI water, and loaded into a 0.5 cc U-100 insulin syringe (28 G ½", Becton Dickinson and Co., Franklin Lakes, NJ, USA). Prepared DDSs were stored at 4°C before injection. The endotoxin study was conducted according to the Pierce Chromogenic Endotoxin Kit (Thermo Scientific, Waltham, MA, USA) on drug-loaded microspheres and microsphere-hydrogel DDS. Based on the published work in monkeys (Bantseev et al., 2019) and rabbits (Bantseev

et al., 2017), acceptable endotoxin level is below 0.5 EU/ml, which is equivalent to 0.025 EU/eye after the 50 μ l intravitreal injection. Only DDS with endotoxin value below 0.025 EU/eye (typical value for our DDS is 0.01 EU/eye) was used for the study. Aflibercept drug release rate and morphological analysis along with our hydrogel material characterization and time-course drug release profiles have been previously detailed (Drapala et al., 2014; Turturro et al., 2011; Liu et al., 2019; Kim et al., 2020; Liu et al., 2019; 2020). The dosage is in accordance with published studies required to reduce VEGF-A-induced endothelial cell proliferation in vitro by 50% (Xu et al., 2013).

Animals

A total of 23 rhesus macaques (*Macaca mulatta*) were used for the study. All animals were born and maintained at the California National Primate Research Center (CNPRC). All NHPs included had normal ophthalmic examinations and were deemed healthy by physical examination and results of complete blood cell counts and serum biochemical analyses. No data was excluded from any animal. Based on a standard power analysis for a two tailed t-test with $\alpha = 0.05$ and Power = 0.8, and in order to assure significance for a difference at an effect size of 0.8 standard deviations, a sample size of at least 3 animals was required.

There were 11 males and 12 females. Mean \pm SD age of the primates was 6.8 ± 1.7 years (range 3–10 years; median 7 years); weight was 10.0 ± 3.4 kg (male: 12.7 ± 3.1 kg, female: 7.8 ± 1.5 kg). The CNPRC is accredited by the Association for Assessment and Accreditation of Laboratory Animal Care (AAALAC) International. The guidelines of the Association for Research in Vision and Ophthalmology Statement for the Use of Animals in Ophthalmic and Vision Research were followed. All studies were in accordance with the National Institutes of Health *Guide for Care and Use of Laboratory Animals*. The injection of aflibercept-DDS and ophthalmic examinations were performed according to an animal protocol that was approved by the Institutional Animal Care and Use Committee at the University of California-Davis.

Twelve animals were allocated to the pharmacokinetic group for the measurement of bioactive aflibercept concentrations in the aqueous, vitreous, and retina. Results of pharmacokinetic analysis will be reported in subsequent publication. Eleven animals were used for the safety and biocompatibility arm. Most animals were monitored short-term (<7 months), but a subset (3 animals) was allocated to long-term (up to 24 months) follow-up. We anticipate human patients to require two intravitreal injections per year. As such, a long-term group was established to evaluate the ocular tolerability and the eye's response to repeat aflibercept-DDS injections. All primates were sedated with ketamine hydrochloride (5–30 mg/kg) and dexmedetomidine (0.0075–0.015 mg/kg) intramuscularly for all procedures. All primate examinations were monitored by a CNPRC veterinarian and trained technician. Pain was controlled with proparacaine 0.5% solution topically if required. Ketoprofen 5 mg/kg IM q24hr prior to IVT-injection then post-op for 3 days was administered.

Post-op therapy also included simbadol 0.72 mg/kg SC q24hr for 3 days and cefazolin 25 mg/kg IM q12hr for 5 days. Atropine 1% solution and bacitracin-neomycin-polymyxin ointment were also administered post IVT-injections. Artificial tear drops were applied to the surface of all eyes during exams and imaging to prevent dryness and provide comfort. NHP eyes were thoroughly washed at completion of exam and imaging parameters and stained with fluorescein to examine for ulceration. Ophthalmic examinations were performed at baseline, the day of IVT aflibercept-DDS injection, and monthly or trimonthly thereafter (animals examined >7 months received 3-month examinations). Advanced imaging and electroretinography were performed at baseline and at monthly/trimonthly examinations. Additional diagnostics (specular microscopy, streak retinoscopy, corneal pachymetry, A-scan biometry) were performed at baseline and endpoint examinations.

Ocular examination and imaging

Ophthalmic examinations were performed in dorsal recumbency with the exception of rebound tonometry, under sedation using intramuscular ketamine as described above. Ophthalmic examinations were performed at baseline and monthly up to 7 months, then every 3 months thereafter for primates with long-term analysis (24 months). Rebound tonometry was used for IOP measurements using the TonoVet rebound tonometer (Icare, Helsinki, Finland). Primates were in a seated position and gentle restraint was used by a secondary operator while the primary operator measured IOP. A total of six consecutive IOP readings were obtained, and the average values were automatically calculated by the Icare device. Consecutive readings with little deviation were considered valid per recommendations by the manufacturer. After IOP measurements were performed, pupillary dilation was achieved using Tropicamide 1% (Bausch & Lomb, Tampa, FL, USA), Phenylephrine 2.5% (Akorn, Lake Forest, IL, USA), and Cyclopentolate 2% (Akorn, Lake Forest, IL, USA). Ophthalmic examinations were then performed using slit-lamp biomicroscopy (SL-17 Biomicroscope, Kowa Company, Japan) and indirect ophthalmoscopy (Keeler VANTAGE Plus; Keeler Inc., Broomall, PA) using a 28 or 2.2D indirect lens (Volk Optical, Inc., Mentor, OH). A semiquantitative preclinical ocular toxicology scoring system (SPOTS) was used for all animals (Eaton et al., 2017). All eyes were photographed at each examination with a digital color camera (Canon EOS5D, flash 1/64, ios 200, F16). At the end of examinations, the cornea was stained with fluorescein (BioGlo, HUB Pharmaceuticals LLC, USA).

Retinal imaging was performed monthly to trimonthly for up to 24 months as previously described (Kim et al., 2020; Lin et al., 2021; Moshiri et al., 2019). In brief, spectral-domain optical coherence tomography (SD-OCT) with confocal scanning laser ophthalmoscopy (cSLO) was performed (Spectralis® HRA+OCT). Red-free and color fundus photographs were acquired with a CF-1 retinal camera using a 50° wide angle lens (Canon, Tokyo, Japan). For fluorescein angiography, intravenous catheters were placed. Metoclopramide 0.5 mg/kg

was administered following intravenous access with slow infusion over 20–30 seconds of 2.5 mg/kg fluorescein injection (AK-Fluor 10%). Following injection, OD images were acquired every 10 seconds for the first minute then every 30 seconds up to 5 minutes followed by imaging OS at the 6-minute timepoint. Eyelid specula were used, and corneal hydration was maintained through application of topical lubrication (Gentle artificial tears) approximately every 2 minutes or frequently as needed during imaging sessions.

Intravitreal injection of aflibercept-DDS

All IVT injections of aflibercept-DDS were performed by a board-certified Diplomate of the American College of Veterinary Ophthalmology (SMT) in the right eye of all NHPs with the left eye serving as an untreated control. With primates sedated, the corneal and conjunctival surfaces were rinsed with 5% povidone iodine and sterile saline solution. The conjunctival fornices were then cleaned with a sterile cotton tipped applicator moistened with 5% povidone iodine solution. Once an eyelid speculum was placed, the target injection site was swabbed with a cotton tipped applicator moistened with 0.5% proparacaine solution to achieve local anesthesia. A sterile aliquot of 50 μ L (Rudeen et al., 2022) containing $\sim 15 \mu$ g of aflibercept was administered via IVT injection in the right eye 2.5 mm posterior to the superior limbus using a 27-gauge hypodermic needle and tuberculin syringe. Anticipating removal of the needle, the injection site was quickly compressed with Colibri forceps, and a cotton tipped applicator to prevent reflux of aflibercept-DDS. Neomycin-polymyxin-bacitracin ophthalmic ointment was instilled after the procedure. A subset of primates ($n=3$) in the biosafety arm received a second injection at 9 months during their 24 months of long-term follow-up.

Full-field electroretinography (ERG)

Following mydriasis, ERG was performed for all animals at baseline, monthly (for the first 7 months, then every 3 months thereafter), and at terminal endpoints. Dark adaptation was performed for 30 minutes while NHPs were monitored under sedation. ERG was performed with the RETevet™ device (LKC Technologies, INC., Gaithersburg, MD) with firmware version 2.11.3. ERG testing consisted of using a flash stimulus at 0.01, 3.0 and 10.0 $\text{cd}\cdot\text{s}/\text{m}^2$ in the dark-adapted state. After 10 minutes in the light-adapted state a flash stimuli of 3.0 $\text{cd}\cdot\text{s}/\text{m}^2$ intensity was used, as well as a 30 Hz photopic flicker. Photopic negative response (PhNR) at minimum and at 72 ms was recorded using a red flash 1.0 $\text{cd}\cdot\text{s}/\text{m}^2$ at 3.4 Hz on a blue background of 10 $\text{cd}\cdot\text{s}/\text{m}^2$. Measurements were recorded and evaluated utilizing the manufacturer's software. Time (ms) and amplitude (μ V) were obtained for each eye for all tests.

SD-OCT and retinal thickness measurements

Using Heidelberg Explorer software (version 1.8.6.0; Heidelberg Engineering), SD-OCT images were obtained for quantitative measurement of retinal layers. The foveal center for each

image was determined where the fovea had the greatest depth. The manufacturer scale was used on SD-OCT images to calibrate ImageJ (Version 1.54i 03) prior to taking manual measurements for each retinal layer. Each retinal layer was measured 1.5 mm nasal and temporal to the foveal center. Additional measurements were taken at the foveal center. Layers measured were retinal nerve fiber layer (RNFL), ganglion cell layer (GCL), inner plexiform layer (IPL), inner nuclear layer (INL), outer plexiform layer (OPL), outer nuclear layer (ONL), photoreceptor inner segments (IS, 'myoid zone'), photoreceptor outer segments (OS), retinal pigmented epithelium (RPE), choriocapillaris (CC), outer choroid (OC), and total retinal thickness (TRT).

Additional diagnostics

Central corneal thickness was measured using ultrasound pachymetry (Pachette 4, DGH Technology Inc., Exton, PA) in both eyes. Streak retinoscopy (Welch-Allyn, Inc. Skaneateles, NY) was performed following cycloplegia and dilation (Tropicamide 1%, Phenylephrine 2.5%, Cyclopentolate 2%) to determine refractive error. Noncontact specular microscopy (Topcon SP-2000P, Topcon Corp., Tokyo, Japan) was performed to evaluate corneal endothelial cell density. Additionally, A-scan ocular biometry (Sonomed Pacsan Plus, Escalon, Wayne, PA) was performed to measure axial globe length (AXL), axial AC depth, lens thickness, and vitreous length. These procedures were performed in both eyes at baseline and humane endpoints for comparison.

Histopathology

Fourteen eyes from seven macaques were enucleated immediately following humane euthanasia (sodium pentobarbital 120 mg/kg IV) and placed into 10% buffered formalin at different timepoints post IVT injection ($n=1$ at 3 months, $n=2$ at 6 months, $n=1$ at 7 months, and $n=3$ at 24 months). Globes were submitted to the Comparative Ocular Pathology Laboratory of Wisconsin for histopathologic analysis as previously described (Kim et al., 2020). Multiple deeper sections of blocks were made in order to adequately sample residual DDS in the vitreous.

Statistical analysis

Statistical analysis was performed using a paired t-test to compare baseline and endpoint data (corneal thickness, endothelial density, axial globe length, refractive error). Significance was set at $P<.05$. Analyses were performed in Microsoft Excel (Microsoft Corporation, Redmond, WA, USA) and GraphPad Prism Version 9.5.0. (GraphPad Software, Boston, MA, USA) For statistical analysis comparing treatments over time, a repeated measures ANOVA using a linear mixed effect model was performed. Eye, or equivalently treatments, and month were specified as fixed effects while subjects were specified as random effects. The linear mixed effect model was fitted using SAS 9.4 (SAS Institute Inc, Cary,

NC, USA) with PROC MIXED and different correlation structures on within-subject residuals (using the REPEATED statement) were compared and selected using AIC. The best fitting correlation structure (for nearly all outcomes) was the Kronecker product between eye and month with unstructured and compound symmetry, respectively. Individual p-values for all end points were adjusted for multiple comparisons by Benjamini-Hochberg procedure to control the false discovery rate (FDR).

Results

Safety and tolerability of aflibercept-DDS

Intravitreal delivery of 50 μ L of aflibercept-DDS was successfully achieved in all NHPs with no immediate complications from the procedure such as lens perforation. Subsequent ocular examinations for 15 NHPs that did not experience adverse events showed symmetrical pupillary light reflexes. The aflibercept-DDS was seen on slit lamp biomicroscopy post-injection in all primates in the anterior superotemporal vitreous in close proximity to IVT injection site (Figure 1). Few vitreous cells (0-4; SPOTS scoring system (Eaton et al., 2017)) were appreciated consisting of predominantly white and occasional pigmented cells up to 9 months post injection; median 2 (1 month), 1 (1-3 months, 6 months), and 0.5 (7-9 months, 5 months). A conglomerate of aflibercept-DDS was visualized in 19/23 NHPs as a white opaque tubular to vermiform immobile structure in the anterior vitreous. Small, fine, white, refractive particles were visualized in 9 of 23 NHPs. In the rhesus macaques with longest follow-up ($n=3$; 24-month endpoint) that received a second injection at 9 months, aflibercept-DDS conglomerates began fragmenting to fine particles around 9 months following first IVT injection. All primates had visible aflibercept-DDS at their final examination prior to euthanasia. Fine particles of the aflibercept-DDS were approximately 1:50 to 1:25 (Figure 5(c)) the size of the optic nerve head diameter and may represent degrading microsphere or hydrogel, while conglomerates ranged from 1:10 to 2x the optic nerve head diameter (1.3 \times 1.8 mm dia (Lin et al., 2021)). Aflibercept-DDS clumping impeded funduscopy in 4/23 NHPs for at least one timepoint. The hydrogel

appearance in the superior dilated pupillary axis was likely related to positioning of the animals during sedation and acquisition of diagnostics. Anterior migration of the aflibercept-DDS was not observed in any NHP.

No significant interaction between month and eye were found after adjusting for multiple comparisons. Hence, main effect for eye was considered for all outcomes. Several outcomes found significant differences, after adjusting for multiple comparisons, for eye (control vs treatment) from the mixed effects analysis. We found that the IOP was slightly decreased in the aflibercept-DDS treated than control eyes (average 14.9 ± 1.7 mmHg, 16.0 ± 1.5 mmHg; respectively) with IOP of treated eyes being on average 1.5 mmHg less than untreated eyes at months 1, 2, 3, 4, 6, 7, and 21 ($P=.004$; Figure 2, Supplementary Table 1) although this difference is not considered clinically relevant. Intraocular pressure ranged from 7 to 25 mmHg in treated and 9 to 25 mmHg in untreated control eyes and were consistent with normal reference values for rhesus macaques (Lin et al., 2021). Furthermore, there was no significant difference in corneal thickness ($492 \pm 39 \mu$ m, $492 \pm 48 \mu$ m; $P=.39$), endothelial density (2523 ± 358 cells/mm², 2749 ± 380 cells/mm²; $P=.58$), axial globe length (20.5 ± 0.8 mm, 20.2 ± 0.9 mm; $P=.37$), or refractive states (0.26 ± 0.9 D, 0.59 ± 0.6 D; $P=.18$) (Figures 3 & 4) in treated vs control eyes, respectively, with values similar to acquired normative data in rhesus macaques (Lin et al., 2021, Casanova et al., 2022, Mitchell et al., 2014). No behavioral changes were noted in NHPs post IVT injection; however, visual acuity testing was not specifically performed.

Preservation of normal retinal morphology and function

Fundus photography appeared normal in all primates at all timepoints although aflibercept-DDS slightly impeded funduscopy in 4 of 23 primates at some time points (1-4 months post injection) (Figure 5). Additionally, we determined that foveal and parafoveal thicknesses of the entire retina and its individual layers as assessed with SD-OCT had mild increased thickness in aflibercept-DDS treated vs controls; however, similarly these differences are not clinically relevant. Specifically, aflibercept-DDS treated eyes show intermittent, mildly increased thickness

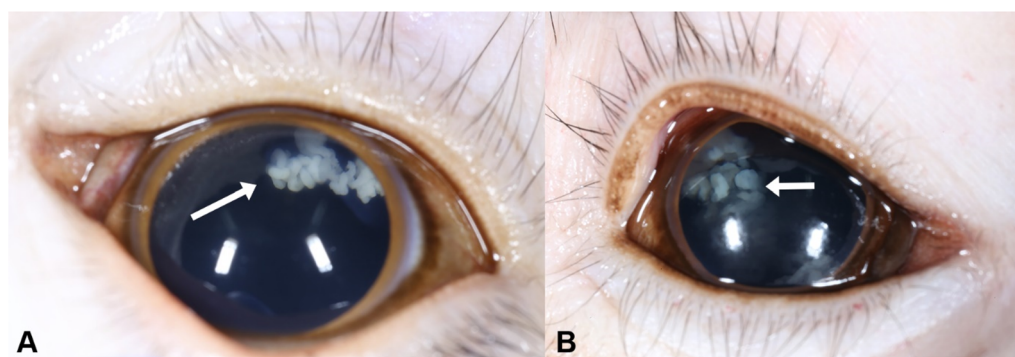


Figure 1. Aflibercept-DDS was visible in the pupillary axis of 4 of 23 rhesus macaques. Representative images of the aflibercept-DDS in the superior vitreous in a (a) 7-year-old male 4 months post IVT injection (b) and in an 8-year-old female 1-month post IVT injection. (b) Note some DDS is appreciated in the inferior vitreous behind the flash artifact. The representative images show the aflibercept-DDS (arrows) in the superior anterior vitreous visible as a white, opaque tubular to vermiform structure.

measurements in the nasal IPL ($8\mu\text{m}$ at 15 months; $P=.002$), nasal ONL (average $6.6\mu\text{m}$ at 1, 5, and 9 months; $P=.02$), nasal TRT (average $8.5\mu\text{m}$ at 1 and 2 months; $P=.02$), temporal IS (average $2.6\mu\text{m}$ at 4 and 15 months; $P=.02$), temporal TRT (average $9\mu\text{m}$ at 1, 8, and 21 months; $P=.02$), foveal GCL (average $6.1\mu\text{m}$ at 7 months; $P=.03$), and foveal RPE (average $0.31\mu\text{m}$; $P=.02$). All other retinal layering measurements showed no statistical differences (Figure 6 & Supplementary Figure 1, 2, 3, and Supplementary Table 2). Additionally, no overt retinal morphologic abnormalities were appreciated at any timepoint, and no retinal or choroïdal vascular abnormalities were detected with fluorescein angiography.

Photopic and scotopic full-field ERG demonstrated normal outer and inner retinal function responses in aflibercept-DDS-treated and untreated control eyes throughout the duration of the study. We found select increased implicit times in aflibercept-DDS treated vs control eyes; however, differences

were considered clinically irrelevant. To illustrate, aflibercept-DDS treated eyes show small increased implicit times at a dark-adapted bright flash test at $3.0\text{cd}\cdot\text{s}/\text{m}^2$ (a-wave, average 4.8ms at 12 and 21 months, $P<.001$; b-wave, average 0.41ms at 1, 4, and 21 months, $P=.02$), dark-adapted bright flash test at $10.0\text{cd}\cdot\text{s}/\text{m}^2$ (a-wave, average 2.2ms at 1 and 12 months; $P=.03$), and light-adapted bright flash test at $3.0\text{cd}\cdot\text{s}/\text{m}^2$ (a-wave, average 0.41ms at 1, 4, 6, and 21 months; $P=.003$). These observations were primarily due to two NHPs that had longer implicit times in the aflibercept-treated eye throughout the study that was also present at baseline. Aflibercept-treated eyes showed a small decrease b-wave implicit time at light-adapted bright flash test at $3.0\text{cd}\cdot\text{s}/\text{m}^2$ with an average of 0.68ms at baseline, 4, 6, 9, 12, 15, and 21 months ($P<.001$). All other ERG parameters showed no significant differences (Figure 7 & Supplementary Figure 4, Supplementary Table 3). Cone flicker response b-wave implicit times ($25.1\pm 0.6\text{ms}$) and amplitudes ($63.5\pm 9.4\mu\text{V}$) did not significantly differ from control values. Similarly, photopic negative response (PhNR) amplitudes at minimum (-6.3 ± 1.9 ; $-6.8\pm 1.6\mu\text{V}$) and 72ms (-4.5 ± 1.7 ; $-4.0\pm 1.4\mu\text{V}$) did not significantly differ in primates at all timepoints demonstrating normal retinal ganglion cell responses (aflibercept-DDS-treated right eye; untreated left eye) (Figure 7). Additional ERG findings including photopic mixed-rod cone and rod responses demonstrated no significant differences between eyes over time (Supplementary Figure 4).

Both globes were submitted for histopathology for seven rhesus macaques – three males 6, 7, and 8 years of age and four females 6, 7, 8, and 10 years of age ($n=1$ at 3 months, $n=2$ at 6 months, $n=1$ at 7 months, and $n=3$ at 24 months). Grossly in the right eye of NHPs, a white homogenous material in the posterior chamber, consistent with the aflibercept-DDS injection, was visible (Figure 8). This round material could be seen attached to the ventral ciliary body or near the posterior lens capsule surface protruding into the anterior vitreous. The aflibercept-DDS was visible as free

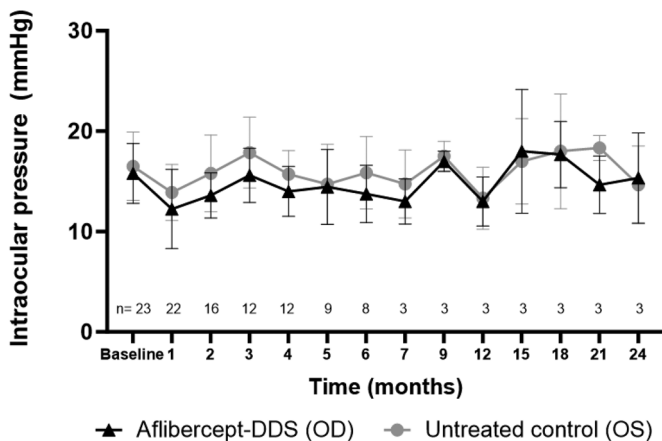


Figure 2. Intraocular pressure did not significantly differ over time or between eyes in 23 NHPs. There was no significant difference in IOPs following IVT injection of aflibercept-DDS to the right eye (OD) where the left eye (OS) served as an untreated control. Mean IOP \pm SD for aflibercept-DDS treated eyes was $14\pm 3\text{mmHg}$ and $16\pm 4\text{mmHg}$ for untreated controls.

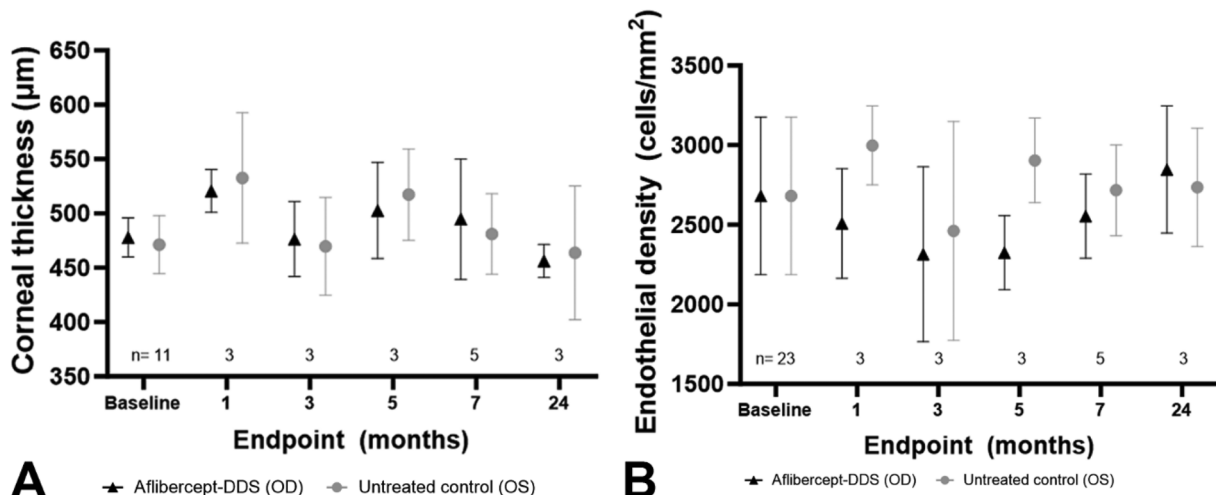


Figure 3. Central corneal thickness and endothelial density did not significantly differ over time or between eyes in NHPs. (a) There was no significant difference ($P=0.86$) in corneal thickness following IVT injection of aflibercept-DDS to the right eye (OD) where the left eye (OS) served as an untreated control. (b) Additionally, there was no significant difference ($P=0.13$) in endothelial density following IVT injection of aflibercept-DDS to the right eye (OD) where the left eye (OS) served as an untreated control.

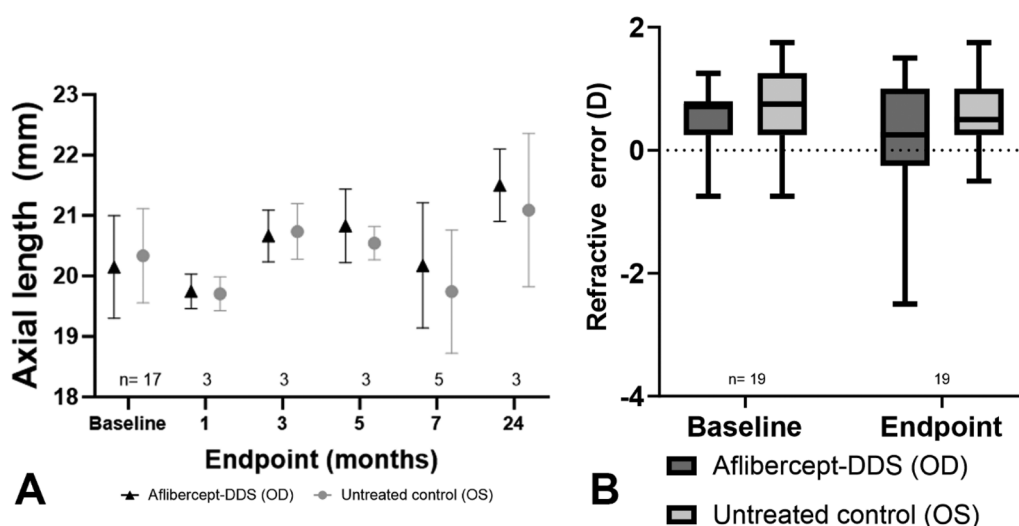


Figure 4. Axial globe length and refractive error did not significantly differ over time or between eyes in NHPs. (a) There was no significant difference ($P=0.42$) in globe length (mm) following IVT injection of aflibercept-DDS to the right eye (OD) where the left eye (OS) served as an untreated control. (b) Additionally, there was no significant difference ($P=0.09$) in refractive error (D) following IVT injection of aflibercept-DDS to the right eye (OD) where the left eye (OS) served as an untreated control.

amorphous basophilic material (aflibercept-DDS) enclosed by a thin fibrous capsule and surrounded by small aggregates of foamy macrophages with intracytoplasmic variably sized lipid material. This cellular reaction associated with the aflibercept-DDS material is consistent with a mild foreign body response to the hydrogel rather than inflammation. No scleral or retinal lesions associated with the intraocular injections were identified. The hydrogel was not observed in the iridocorneal angle in NHPs. The untreated left eye showed normal morphology in all macaques.

Adverse events

A serious adverse event (SAE) occurred unexpectedly in a 7-year-old male NHP two days after IVT injection. This event occurred in the first injected primate early on. Following IVT injection mild diffuse corneal edema, corneal ulceration, and severe fibrin and white blood cells filled the whole anterior chamber. The posterior segment exam was impossible due to anterior segment changes. Severe diffuse conjunctival inflammation was appreciated with a focal conjunctival swelling around the needle tract at the 11 o'clock position. Intravitreal injection was routine in this NHP and the inflammatory event occurred within 24 hours. Topical and systemic corticosteroids were initiated but unfortunately the inflammation remained severe with secondary elevation in intraocular pressure (82 mmHg) and humane euthanasia was performed 72 hours post injection. Histopathology was consistent with either a severe endophthalmitis, or toxic anterior segment syndrome (TASS) reaction and a thorough review of DDS synthesis was conducted. It was suspected that contamination of core deionized water with endotoxin precipitated the event. Due to these events multiple measures were performed to decrease the risk of TASS which included: use of bottled autoclaved DI water, disposal of all open materials, fabrication of DDS and microparticles under sterile laminar hoods, switching to single use disposable equipment (when

applicable), and conducting endotoxin testing on microparticles and DDS. Other preventative measurements included: recording lot numbers for all ocular medications given to primates that received IVT injections, allowing a contact time of 5 minutes for the 5% povidone iodine solution, and having two investigators verify that there is no water in the syringe case. Additional SAE's have not been observed to date.

A total of eleven primates experienced mild to moderate TASS. Multiple NHPs were affected simultaneously due to batch injections. Five events, three events, and an additional three events all occurred due to the same batch of injections. Two primates were affected with the NHP that experienced SAE; however, their clinical signs were mild in comparison. Required therapies included 0.2-0.4 mg intravitreal dexamethasone and 0.2-0.8 mg subconjunctival dexamethasone (3/11), 0.4 mg intravitreal dexamethasone only (3/11), 0.6 mg subconjunctival dexamethasone only (1/11), 1 mg intravitreal vancomycin (3/11), 2 mg/kg intramuscular dexamethasone (4/11), 25 mg/kg intramuscular cefazolin (2/11), or none (2/11). The majority of clinical signs included conjunctival hyperemia (4/11), corneal edema (4/11), aqueous flare (3/11), aqueous (5/11) and vitreal cell (4/11). Two primates were noted to have fibrinous uveitis. All primates made a complete recovery within 14 days (Figure 9). Histopathology was performed for one primate with similar findings to non-TASS animals (Figure 8). There was clinical concern for posterior cataract formation in this animal, however, upon histologic evaluation, the DDS aflibercept-DDS was appreciated carpeting the posterior lens capsule and no cataract formation was observed. A definitive cause for TASS was never determined and presumed to be batch dependent.

Discussion

In this study, we demonstrated the long-term safety and biocompatibility of a biodegradable aflibercept-DDS in NHPs.

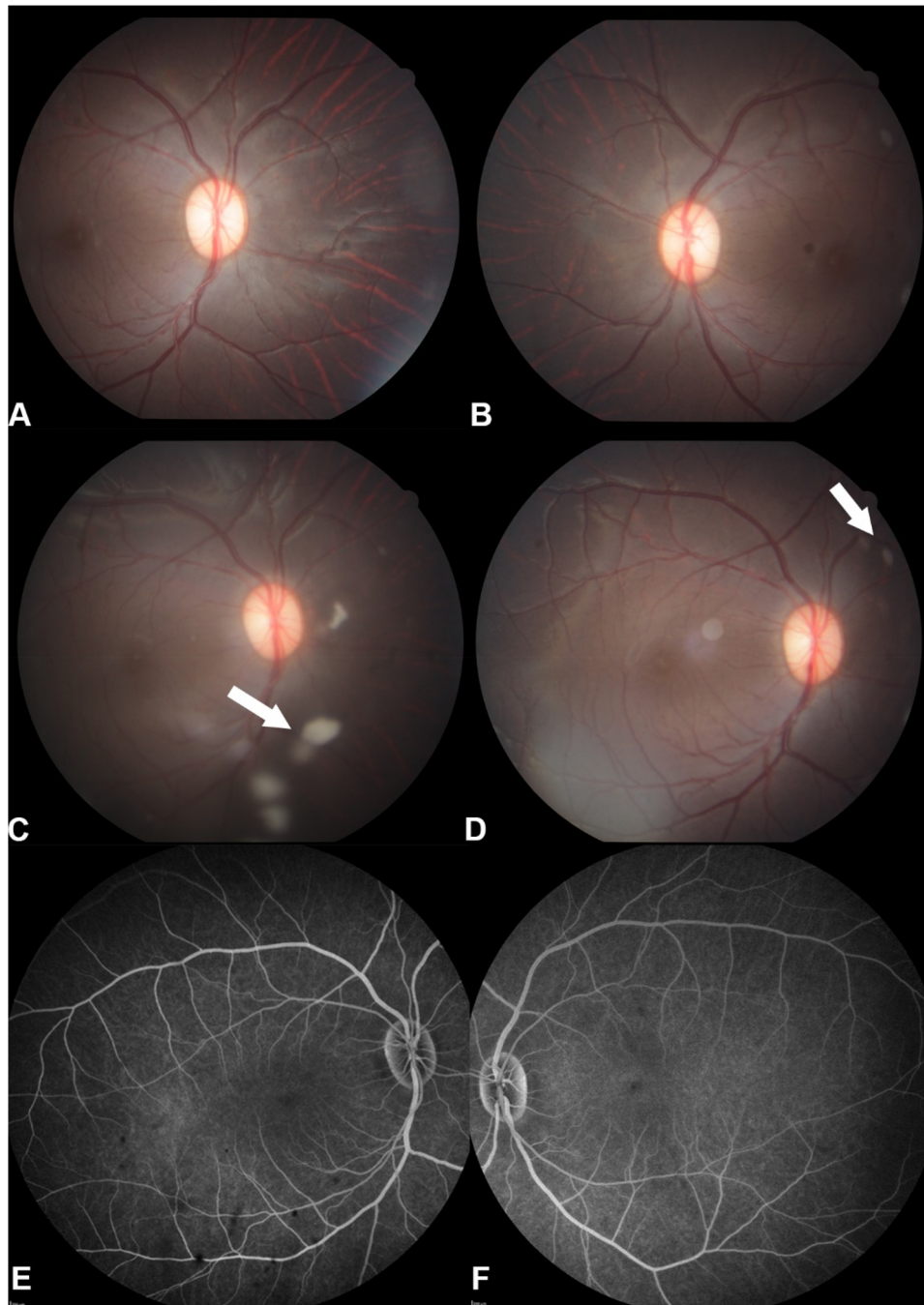


Figure 5. Fundoscopy and fluorescein angiography were largely unremarkable in NHPs receiving aflibercept-DDS as illustrated in representative images of an 8-year-old male. Fundoscopy was unremarkable post IVT when comparing (a) aflibercept-DDS treated and (b) untreated control eyes (a second IVT was administered at 9 months) at final endpoint of 24 months. Four of 23 NHPs had aflibercept-DDS impede funduscopy to varying degrees as illustrated in (c) 18 months post IVT injection and in (d) 6 months later showing less aflibercept-DDS (white arrows). (e) and (f) demonstrate normal fluorescein angiography 24-months post IVT in (e) aflibercept-DDS treated and (f) untreated control eyes.

The hydrogel used in the present study was fabricated to be fully biodegradable without altering transition temperatures via incorporation of poly (L-lactic acid)-polyethylene glycol diacrylate (PLLA-PEG-DA) (Drapala et al., 2014). The process of biodegradation leads to conversion of the polymeric network into a nontoxic, lower molecular weight end product, which avoid the need for surgical removal from the vitreous. This work extends upon our previous pilot study demonstrating the short-term biocompatibility and pharmacokinetics of a non-biodegradable aflibercept-DDS in rhesus macaques (Kim

et al., 2020). This system consisted of biodegradable poly-lactic-co-glycolic acid (PLGA) microspheres suspended within a nondegradable thermo-responsive injectable hydrogel in order to observe histological changes and achieved sustained release of loaded aflibercept for at least 6 months. Our current study provides the safety and tolerability of an intravitreal PLGA microsphere drug delivery platform in rhesus macaques over two-year period further expanding on the use of PLGA microspheres in retinal and other ocular diseases (Herrero-Vanrell et al., 2014).

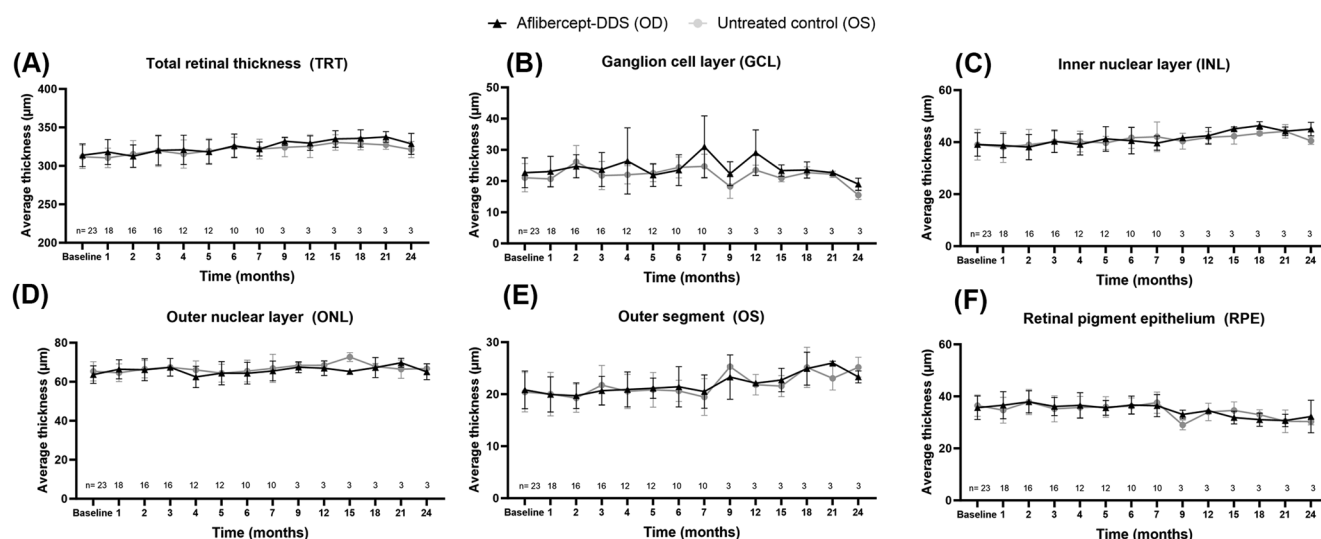


Figure 6. Thickness of the entire retina as well as selected retinal layers as assessed with SD-OCT did not clinically differ over time between aflibercept-DDS versus untreated control eyes. Measurements 1.5mm temporal to the fovea of total retinal thickness a), as well as select retinal layers (B, ganglion cell layer; C, inner nuclear layer; D, outer nuclear layer; E, outer segment; and F, retinal pigmented epithelium) in the aflibercept-DDS (right eye, black line) and untreated control eye (left eye, gray line) were measured up to 24months with no clinically significant difference between groups and timepoints using a Welch's t-test. Additional temporal measurements as well as measurements through the fovea and 1.5mm nasal to the fovea are available for review in [Supplementary Figures 1, 2, and 3](#).

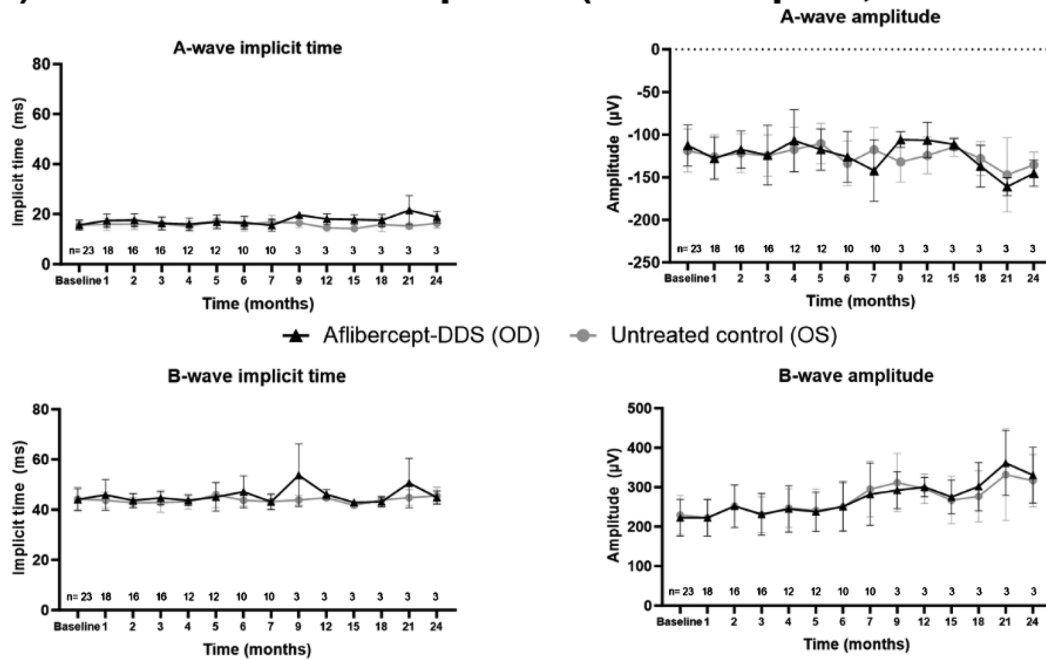
One of the biggest burdens on patients currently being treated with IVT anti-VEGF agents is the need for repeated injections. Degradable PLGA microspheres embedded in degradable PEG-PLLA-DA/NIPPAM hydrogels are capable of sustained aflibercept release for ~6months (Liu et al., 2019). The microspheres in the present study were purposefully designed to dissolve in 6months (Liu et al., 2019; Liu et al., 2020), faster rate than the hydrogel, to ensure that the drug is completely released from the microspheres. By 9months post IVT, the hydrogel was fragmented and almost completely biodegraded. A superior IVT injection was selected to visually monitor the aflibercept-DDS degradation over time. The aflibercept-DDS could be appreciated superiorly in the dilated pupillary axis only in 18% of the NHPs (Figures 1 and Lanzetta et al., 2024(c)) suggesting that it remained close to the injection site in most NHPs. Occasional hydrogel appearance in the superior dilated pupillary axis was likely related to NHP positioning during sedation and acquisition of diagnostics when exams were performed. No primate had grossly visible hydrogel on non-dilated examination. Nevertheless, inferior IVT injections of the aflibercept-DDS would be optimal in clinical patients to prevent presence of the material in the pupillary axis and concomitant visual anomalies.

The aflibercept-DDS was observed in most NHPs suspended in the anterior superotemporal vitreous on dilated examination of the fundus. It was intentionally administered in the superior vitreous so that migration of the aflibercept-DDS could be monitored over time as unconstrained particle migration can be associated with glaucoma and intraocular inflammation (Adamson et al., 2016). The DDS in the present study was designed with microspheres of 8μm average diameter embedded in a thermo-responsive hydrogel (Osswald and Kang-Mieler, 2015; Rudeen et al., 2022) that facilitates localization of the microspheres near the injection site, prevents migration, and extends the release profile from ~154days with PLGA microspheres alone (Osswald and Kang-Mieler, 2015) to >200days when hydrogel embedded

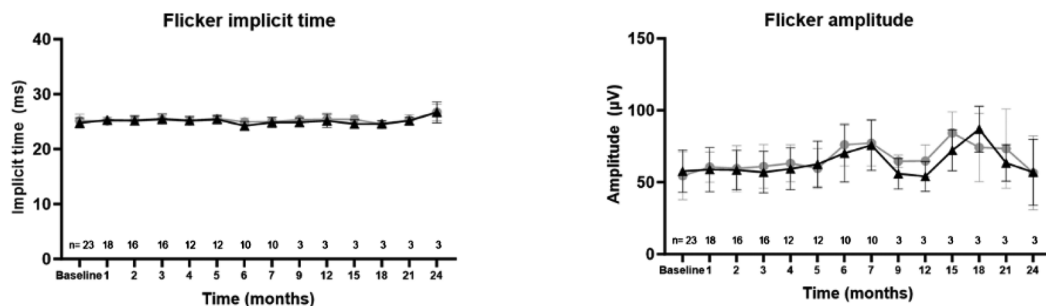
(Liu et al., 2019). Based on our earlier work (Liu et al., 2020), this size led to adequate release profile and prevented particle migration outside the hydrogel network. Indeed, the lack of inflammation observed in the present study coupled with the optimization of hydrogel crosslink density with a radius of gyration of the hydrogel being ~17nm (Osswald and Kang-Mieler, 2015) ensures microspheres did not migrate and diffuse sporadically out of the hydrogel and is an important reason for the lack of any long-term inflammation observed in the present study. Migration of IVT anti-VEGF agents and microparticles have been reported to induce anterior segment inflammation (Adamson et al., 2016; Mozayan and Farah, 2013). Particle migration can happen readily in NHPs due to ciliary changes during disaccommodation, allowing microsphere migration from the vitreous to the anterior chamber due to fluid flow (Lütjen-Drecoll et al., 2010; Croft et al., 2013; 2013). In the current study, anterior migration of aflibercept-DDS and anterior uveitis was absent in all NHPs. Additionally, administration of the DDS was smooth with no complications during the IVT injection such as cataract, retinal tear and detachment, or vitreous hemorrhage.

In the present study, aflibercept-DDS did not elicit an inflammatory response when injected into the vitreous cavity apart from a mild foreign body reaction likely associated with the degrading hydrogel. We highlight that this foreign body response was localized to the hydrogel and did not lead to cataract or impact the adjacent retina. These results were consistent with the excellent safety profile observed in our initial study of a non-biodegradable aflibercept-DDS in NHPs (Kim et al., 2020). The reaction is markedly less than a previous study following IVT administration of PLGA rods in cynomolgus monkeys where retinal degeneration and epiretinal membranes were observed (Booler et al., 2021). Similarly, in a study evaluating microparticles loaded with two different anti-VEGF domain antibodies, anterior segment inflammation, microparticle dispersion in the ventral iridocorneal angle, perivascular sheathing, and blood retinal barrier breakdown

A) Mixed rod-cone response (dark-adapted, 3.0 cd•s/m²)



B) Cone flicker response (light-adapted, 3.0 cd•s/m²)



C) Photopic negative response (PhNR)

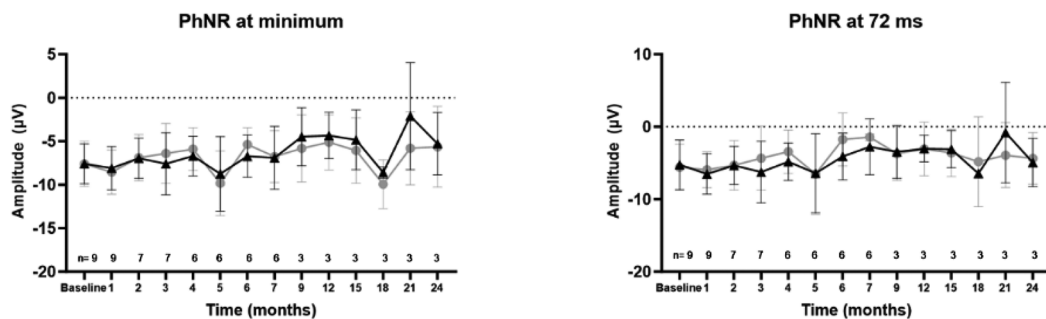


Figure 7. Scotopic full-field electroretinography, cone flicker, and photopic negative response demonstrated normal retinal function throughout the study period. There were no clinically significant differences over time or between aflibercept-DDS (right eye) versus the untreated control eyes (left eye). (a) Dark adaptation: 3.0 cd•s/m², chromaticity (0.33, 0.33) at 0.05 Hz, background 0.0 cd/m². (b) Light adaptation: 3.0 cd•s/m², chromaticity (0.33, 0.33) at 28.3 Hz; background: 30 cd/m², chromaticity (0.33, 0.33). (c) Photopic negative response (PhNR) red flash 1.0 cd•s/m² at 3.4 Hz on a blue background of 10 cd/m².

were observed necessitating veterinarian intervention in some cases (Adamson et al., 2016). A single NHP experienced a SAE in the present study presumably due to contamination of deionized water with endotoxin. Toxic anterior segment syndrome was documented in 11 NHPs which all responded favorably to medical therapy. The underlying etiology of TASS

is seldom found clinically. Sengupta and colleagues demonstrated that in 51.7% of TASS cases no etiology was found despite a careful search (Sengupta et al., 2011). Some potential causes include inadequate cleaning of surgical instruments, contamination of surgical instruments, or adverse drug reactions (Park et al., 2018). Although surgery with

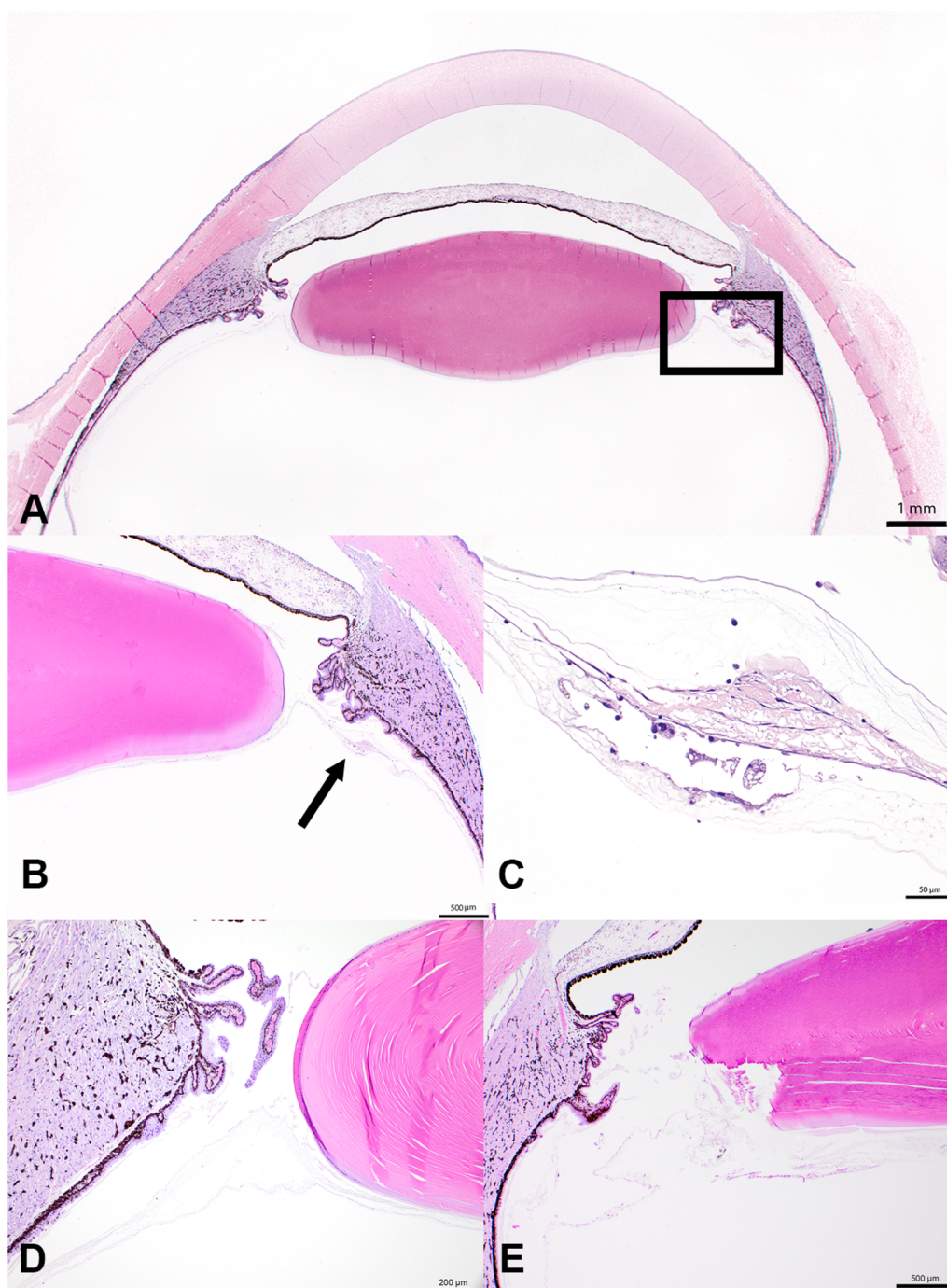


Figure 8. Histopathology showed no cataract formation, retinal detachment, or uveitis in any NHP. Histopathologic images A), B), and C) of the right globe of an 11-year-old female rhesus macaque 3 at months post-IVT injection of aflibercept-DDS that experienced TASS. A) At low magnification a small aggregate of homogeneous material can be seen in the anterior vitreous immediately posterior to the lens capsule and adjacent to the ciliary bodies. The black box in figure A) represents magnified views captured in B) and C). At higher magnification B) and C), the smaller aggregates are foamy macrophages admixed with fusiform cells forming membranes and clusters in the superior vitreous chamber attached to the ciliary body surface and to a lesser extent, carpeting the posterior lens capsule B) that clinically resembled small posterior capsular cataract formation. The cells are surrounded amorphous to non-staining material interpreted as the aflibercept-DDS. The rest of the globe presented in a near normal appearance. Representative images of a 7-year-old female 7 months D) and an 8-year-old male 24 months E) post IVT injection of aflibercept-DDS showing a well-delineated accumulation of light basophilic, amorphous to granular material (aflibercept-DDS) along with small numbers of macrophages in the anterior vitreous adjacent to the ciliary body pars plana, peripheral retina, and posterior lens capsule.

phacoemulsification is most commonly associated with TASS, intravitreal injections are frequently reported to cause sterile inflammatory reactions with both aflibercept and bevacizumab being described in past outbreaks (Wickremasinghe et al., 2008; Sato et al., 2010; Fielden et al., 2011; Kay et al., 2011; Wang et al., 2013; Goldberg et al., 2014; Orozco-Hernández et al., 2014; Hahn et al., 2015; Greenberg

et al., 2019). In the current study, the underlying cause of TASS was unclear but it was unlikely to be a reaction to the DDS given that all NHPs recovered fully and only required transient steroids. Indeed, the histopathology from NHPs experiencing TASS was similar to those that did not (Figure 8).

A limitation with thermoresponsive hydrogels and hydrogels that experience swelling initial burst (IB). Initial burst

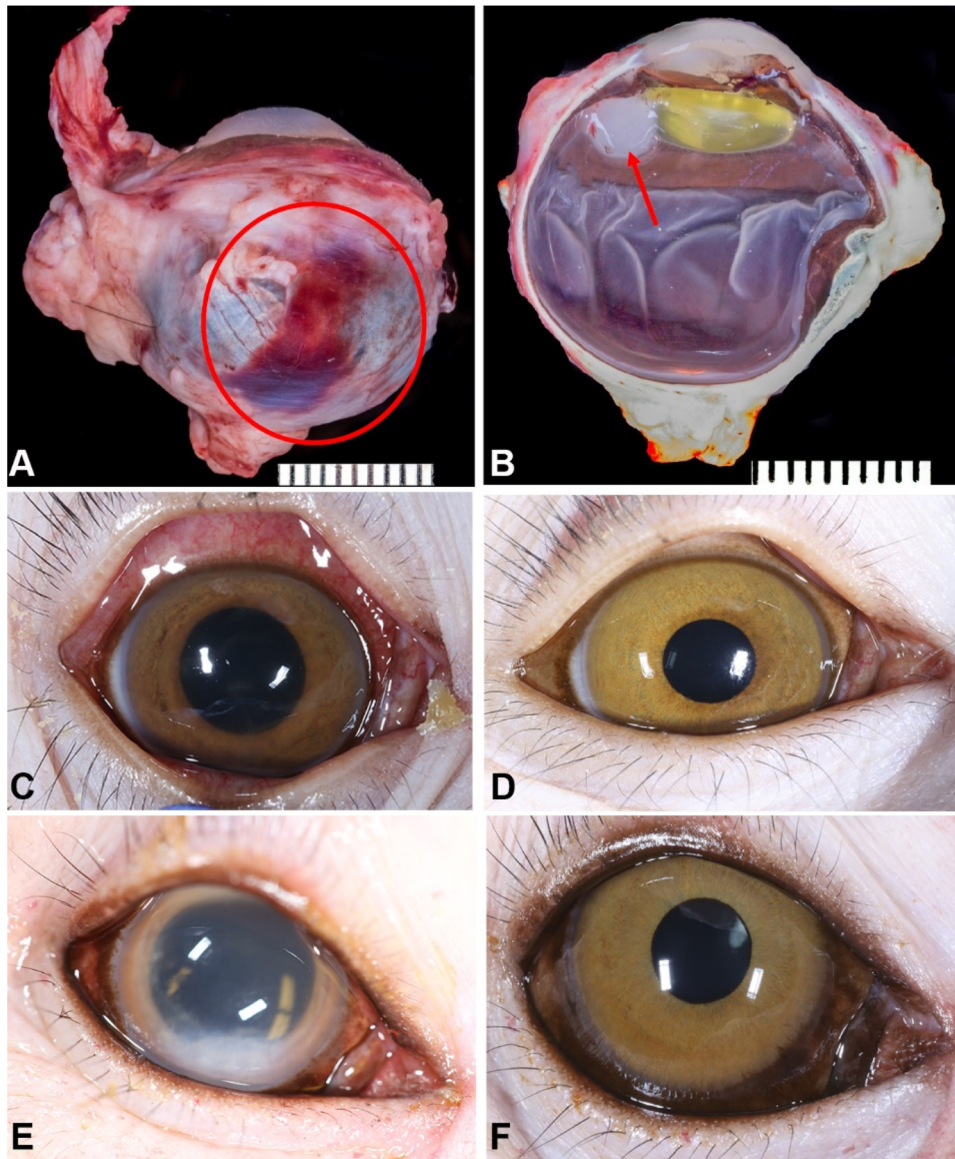


Figure 9. Adverse events: a serious adverse event (SAE) occurred in one NHP and 11 of 23 NHPs experienced mild to moderate toxic anterior segment syndrome (TASS) that responded to anti-inflammatory treatment. A focally extensive area (circle) of subconjunctival and episcleral hemorrhage adjacent to the injection site (a) with focal accumulation of pale material (aflibercept-DDS, arrow) in the superior posterior chamber is seen in a 7-year-old male rhesus macaque that experienced a SAE two days post IVT aflibercept-DDS injection in the right eye. Histologic analysis demonstrated neutrophilic episcleritis, bulbar conjunctivitis, endophthalmitis (idiopathic), anterior uveitis, and papillitis. Gram's stains for bacteria failed to reveal microorganisms. TASS ranged from mild (C) to moderate (E). (c) 6-year-old male three days post IVT injection demonstrating mild TASS characterized by subconjunctival hemorrhage, conjunctival hyperemia, corneal edema, and fibrinous uveitis in the right eye. (d) The same 6-year-old male 3 weeks post IVT injection. (e) 10-year-old female two days post IVT injection demonstrating moderate TASS characterized by corneal edema, 4+ anterior chamber flare and white blood cell, with fibrinous uveitis adhered to the lens capsule in the right eye. (f) The same 10-year-old female 3 weeks post IVT injection.

from microparticles can be reduced but not eliminated by hydrogels. However, this may not be entirely detrimental as the IB may act as a loading dose during the beginning of treatment. We have previously observed a rapid release of radiolabeled aflibercept from the aflibercept-DDS over the first week, followed by a near zero-order release profile 6 months thereafter (Liu et al., 2019).

Intraocular pressure ranged from 7 to 25 mmHg in treated and 9 to 25 mmHg in untreated control eyes and did not show clinically important differences from baseline or between eyes over the duration of the study with the exception of the single NHP experiencing a SAE. Similarly, detailed assessment of retinal morphology and function with SD-OCT and ERG showed no clinically relevant changes over time or between eyes

demonstrating excellent long-term biocompatibility of this aflibercept-DDS. Mild statistically significant changes were seen in IOP, SD-OCT measurements, and ERG implicit times, however, these changes are likely idiosyncratic and unlikely due to any direct effect of the aflibercept-DDS. Previously, anti-VEGF DDS (ranibizumab or aflibercept) showed a mild but insignificant rise in IOP that did not change over time in Long-Evans male rats treated with aflibercept-DDS and normal preservation of retinal function as assessed by ERG (Osswald et al., 2017). Finally, no retinal or choroidal vascular abnormalities were detected with fluorescein angiography and no change to the ocular biometry, anterior segment parameters (endothelial density and central corneal thickness), or refractive error were observed in the aflibercept-DDS treated eyes. To the author's knowledge, this is

the first long-term study extensively evaluating multiple ocular safety parameters in NHPs with an aflibercept-DDS.

There are significant advantages of using microspheres embedded in biodegradable hydrogels for intraocular delivery of pharmaceuticals. Patient specific implications include intraocular injection via a small gauge needle, lack of general anesthesia and a tolerable outpatient procedure. The hydrogel additionally helps confine the microspheres to the vitreous cavity, promotes an extended-release time, and has a thermoresponsive nature such that it solidifies at body temperature to limit migration into the visual axis. Indeed, previous studies have shown the intravitreal injections of non-hydrogel embedded microspheres of particle sizes greater than accomplished in our current study elicited a robust inflammatory response following injection in rabbits and NHPs (Thackaberry et al., 2017).

Future studies will focus on multiple drug incorporation, evaluation in NHP models of choroidal neovascularization, and pharmacokinetics. Our previous research has shown vitreous aflibercept concentrations well above the reported IC50 for human umbilical vein endothelial cells in NHPs for up to 6 months, demonstrated reduction in choroidal neovascularization, and outlined the release of our aflibercept-DDS in vitro (Liu et al., 2019, Kim et al., 2020, Liu et al., 2020). In the future, we will validate the aflibercept-DDS in a nonhuman primate model of choroidal neovascularization (CNV) will be required prior to clinical trials as well as establishing the pharmacokinetics. However, recently we documented significant decrease in CNV lesion area in Long-Evans rats treated with aflibercept-DDS compared to no treatment for 6 months with a nonsignificant additional ~7% decrease compared to bimonthly bolus aflibercept (Liu et al., 2020). Further molecular testing such as protein and gene expression will also be performed to fully understand the biocompatibility of the DDS.

Conclusion

Intravitreal injection of a biodegradable aflibercept-DDS was safe and well tolerated in NHPs up to 24 months. The aflibercept-DDS was visualized in the vitreous up to 9 months post injection. No consistent differences in clinical examination, ocular imaging, or electrophysiological data were appreciated in treated vs control eyes. Histopathology showed a mild foreign body reaction but no evidence of uveitis, retinal degeneration, or cataract. Future studies are required to test the efficacy of this aflibercept-DDS in a NHP model of choroidal neovascularization.

Disclosure statement

B.D. Story, None; **S. Park**, None; **K. Roszak**, None; **J. Shim**, None; **M. Motta**, None; **M. Ferneding**, None; **K.M. Rudeen**, None; **A. Blandino**, None; **M. Ardon**, None; **S. Le**, None; **L.B.C. Teixeira**, None; **G. Yiu**, None; **W.F. Mieler**, None; **S.M. Thomasy**, None; **J.J. Kang-Mieler**, microsphere thermo-reponsive drug delivery system (P).

Ethical approval

The CNPRC is accredited by the Association for Assessment and Accreditation of Laboratory Animal Care (AAALAC) International. The

guidelines of the Association for Research in Vision and Ophthalmology Statement for the Use of Animals in Ophthalmic and Vision Research were followed. All studies were in accordance with the National Institutes of Health *Guide for Care and Use of Laboratory Animals*. The animal experiments were also conducted following ARRIVE guidelines. Based on a standard power analysis for a two tailed t-test with $\alpha = 0.05$ and Power = 0.8, we estimated the number of samples needed for a given range of effect size (from 0.8 to 1.5 standard deviations of the ERG measurement). In order to assure significance for a difference at an effect size of 0.8 standard deviations, we required a sample size of 3 animals. We added an additional 3 animals to be used for a long-term 2 year follow up. NHPs were provided paired indoor housing and daily animal husbandry was provided by vivarium staff at the CNPRC. NHPs were fed twice a day given at least 20 minutes to feed prior to routine cleaning procedures. Seven biscuits per feeding of 25% protein Monkey Chow were fed to NHPs. Regarding potential pain following IVT-injections, ketoprofen 5 mg/kg IM q24hr prior to IVT-injection then post-op for 3 days was administered. Post-op therapy also included simbadol 0.72 mg/kg SC q24hr for 3 days and cefazolin 25 mg/kg IM q12hr for 5 days. Atropine 1% solution and bacitracin-neomycin-polymyxin ointment were also administered post IVT-injections. Artificial tear drops were applied to the surface of all eyes during exams and imaging to prevent dryness and provide comfort. NHP eyes were thoroughly washed at completion of exam and imaging parameters and stained with fluorescein to examine for ulceration. Animals were then observed for signs of ocular discomfort such as squinting, rubbing, redness or discharge. If this occurred, the PI examined the animal and consulted with CNPRC veterinarian(s) regarding appropriate treatment. Humane euthanasia was performed using sodium pentobarbital 120 mg/kg IV. IACUC approval number 22789.

Author contributions

S.M.T., J.J.K, G.Y., and W.F.M. designed and supervised experiments. B.D.S, S.P., K.R., J.S., M.M., and M.F. performed animal examinations and data collection. M.A. and S.L. processed and stored animal data. A. B. performed statistical analysis. L.B.C.T. conducted histopathologic analysis. B.D.S analyzed all data and drafted the manuscript. All listed authors have reviewed and are in agreement with the published version of the manuscript and agree to be accountable for all aspects of the work.

Funding

Supported by the National Institutes of Health (NIH) R01 EY029298 (JKM), U24 EY029904 (SMT), R01 EY033733 (SMT) and P30 EY12576. Additional support for this work came from the California National Primate Research Center Base Grant from the NIH, Office of Director, OD011107.

Data availability statement

The data that support the findings of this study are available from the corresponding authors, Jennifer Kang-Mieler and Sara Thomasy upon request.

References

- Adamson P, Wilde T, Dobrzynski E, et al. (2016). Single ocular injection of a sustained-release anti-VEGF delivers 6 months pharmacokinetics and efficacy in a primate laser CNV model. *J Control Release* 244:1–13. doi: 10.1016/j.jconrel.2016.10.026.
- Anand AJ, Huang HJ, Hean HH, et al. (2023). Anti-angiogenic carbon nanovesicles loaded with bevacizumab for the treatment of age-related macular degeneration. *Carbon* 201:362–70. HT. doi: 10.1016/j.carbon.2022.09.045.

- Bantseev V, Miller PE, Bentley E, et al. (2017). Determination of a no-observable effect level for endotoxin following a single intravitreal administration to dutch belted rabbits. *Invest Ophthalmol Vis Sci* 58:1545–52. doi: [10.1167/iov.16-21356](https://doi.org/10.1167/iov.16-21356).
- Bantseev V, Miller PE, Nork TM, et al. (2019). Determination of a no-observable effect level for endotoxin following a single intravitreal administration to cynomolgus monkeys. *J Ocul Pharmacol Ther* 35:245–53. doi: [10.1089/jop.2018.0149](https://doi.org/10.1089/jop.2018.0149).
- Booler H, Larsen T, Shelton A, et al. (2021). Foreign body reaction, retinal degeneration, and epiretinal membranes associated with intravitreal administration of PLGA rods. *Toxicol Pathol* 49:656–62. doi: [10.1177/0192623320948851](https://doi.org/10.1177/0192623320948851).
- Brown DM, Michels M, Kaiser PK, et al. (2009). Ranibizumab versus verteporfin photodynamic therapy for neovascular age-related macular degeneration: two-year results of the ANCHOR study. *Ophthalmology* 116:57–65 e5. doi: [10.1016/j.ophtha.2008.10.018](https://doi.org/10.1016/j.ophtha.2008.10.018).
- Casanova MI, Young LJ, Park S, et al. (2022). Normal corneal thickness and endothelial cell density in rhesus macaques (*Macaca mulatta*). *Transl Vis Sci Technol* 11:23. doi: [10.1167/tvst.11.9.23](https://doi.org/10.1167/tvst.11.9.23).
- Chandra S, Arpa C, Menon D, et al. (2020). Ten-year outcomes of anti-vascular endothelial growth factor therapy in neovascular age-related macular degeneration. *Eye (Lond)* 34:1888–96. doi: [10.1038/s41433-020-0764-9](https://doi.org/10.1038/s41433-020-0764-9).
- Croft MA, McDonald JP, Katz A, et al. (2013). Extralenticular and lenticular aspects of accommodation and presbyopia in human versus monkey eyes. *Invest Ophthalmol Vis Sci* 54:5035–48. doi: [10.1167/iov.12-10846](https://doi.org/10.1167/iov.12-10846).
- Croft MA, Nork TM, McDonald JP, et al. (2013). Accommodative movements of the vitreous membrane, choroid, and sclera in young and presbyopic human and nonhuman primate eyes. *Invest Ophthalmol Vis Sci* 54:5049–58. doi: [10.1167/iov.12-10847](https://doi.org/10.1167/iov.12-10847).
- Drapala PW, Jiang B, Chiu YC, et al. (2014). The effect of glutathione as chain transfer agent in PNIPAAm-based thermo-responsive hydrogels for controlled release of proteins. *Pharm Res* 31:742–53. doi: [10.1007/s11095-013-1195-0](https://doi.org/10.1007/s11095-013-1195-0).
- Eaton JS, Miller PE, Bentley E, et al. (2017). The SPOTS system: an ocular scoring system optimized for use in modern preclinical drug development and toxicology. *J Ocul Pharmacol Ther* 33:718–34. doi: [10.1089/jop.2017.0108](https://doi.org/10.1089/jop.2017.0108).
- El Sanharawi M, Kowalczyk L, Touchard E, et al. (2010). Protein delivery for retinal diseases: from basic considerations to clinical applications. *Prog Retin Eye Res* 29:443–65. doi: [10.1016/j.preteyeres.2010.04.001](https://doi.org/10.1016/j.preteyeres.2010.04.001).
- Fielden M, Nelson B, Kherani A. (2011). Acute intraocular inflammation following intravitreal injection of bevacizumab—a large cluster of cases. *Acta Ophthalmol* 89:e664–5–e665. doi: [10.1111/j.1755-3768.2010.02054.x](https://doi.org/10.1111/j.1755-3768.2010.02054.x).
- Flaxel CJ, Adelman RA, Bailey ST, et al. (2020). Age-related macular degeneration preferred practice pattern(R). *Ophthalmology* 127:P1–P65. doi: [10.1016/j.ophtha.2019.09.024](https://doi.org/10.1016/j.ophtha.2019.09.024).
- Goldberg RA, Shah CP, Wiegand TW, Heier JS. (2014). Noninfectious inflammation after intravitreal injection of aflibercept: clinical characteristics and visual outcomes. *Am J Ophthalmol* 158:733–7 e1. doi: [10.1016/j.ajo.2014.06.019](https://doi.org/10.1016/j.ajo.2014.06.019).
- Greenberg JP, Belin P, Butler J, et al. (2019). Aflibercept-related sterile intraocular inflammation outcomes. *Ophthalmol Retina* 3:753–9. doi: [10.1016/j.oret.2019.04.006](https://doi.org/10.1016/j.oret.2019.04.006).
- Hahn P, Chung MM, Flynn HW, Jr., et al. (2015). Postmarketing analysis of aflibercept-related sterile intraocular inflammation. *JAMA Ophthalmol* 133:421–6. doi: [10.1001/jamaophthalmol.2014.5650](https://doi.org/10.1001/jamaophthalmol.2014.5650).
- Heier JS, Brown DM, Chong V, et al. (2012). Intravitreal aflibercept (VEGF trap-eye) in wet age-related macular degeneration. *Ophthalmology* 119:2537–48. doi: [10.1016/j.ophtha.2012.09.006](https://doi.org/10.1016/j.ophtha.2012.09.006).
- Heier JS, Khanani AM, Quezada Ruiz C, et al. (2022). Efficacy, durability, and safety of intravitreal faricimab up to every 16 weeks for neovascular age-related macular degeneration (TENAYA and LUCERNE): two randomised, double-masked, phase 3, non-inferiority trials. *Lancet* 399:729–40. doi: [10.1016/S0140-6736\(22\)00010-1](https://doi.org/10.1016/S0140-6736(22)00010-1).
- Herrero-Vanrell R, Bravo-Osuna I, Andres-Guerrero V, et al. (2014). The potential of using biodegradable microspheres in retinal diseases and other intraocular pathologies. *Prog Retin Eye Res* 42:27–43. doi: [10.1016/j.preteyeres.2014.04.002](https://doi.org/10.1016/j.preteyeres.2014.04.002).
- Holmkvist AD, Friberg A, Nilsson UJ, Schouenborg J. (2016). Hydrophobic ion pairing of a minocycline/Ca(2+)/AOT complex for preparation of drug-loaded PLGA nanoparticles with improved sustained release. *Int J Pharm* 499:351–7. doi: [10.1016/j.ijpharm.2016.01.011](https://doi.org/10.1016/j.ijpharm.2016.01.011).
- Jian HJ, Anand A, Lai JY, et al. (2024). Ultrahigh-efficacy VEGF neutralization using carbonized nanodonuts: implications for intraocular anti-angiogenic therapy. *Adv Healthc Mater* 13:e2302881. doi: [10.1002/adhm.202302881](https://doi.org/10.1002/adhm.202302881).
- Kang-Mieler JJ, Osswald CR, Mieler WF. (2014). Advances in ocular drug delivery: emphasis on the posterior segment. *Expert Opin Drug Deliv* 11:1647–60. doi: [10.1517/17425247.2014.935338](https://doi.org/10.1517/17425247.2014.935338).
- Kay CN, Tarantola RM, Gehrs KM, et al. (2011). Uveitis following intravitreal bevacizumab: a non-infectious cluster. *Ophthalmic Surg Lasers Imaging* 42:292–6. doi: [10.3928/15428877-20110603-04](https://doi.org/10.3928/15428877-20110603-04).
- Kim S, Kang-Mieler JJ, Liu W, et al. (2020). Safety and biocompatibility of aflibercept-loaded microsphere thermo-responsive hydrogel drug delivery system in a nonhuman primate model. *Transl Vis Sci Technol* 9:30. doi: [10.1167/tvst.9.3.30](https://doi.org/10.1167/tvst.9.3.30).
- Lanzetta P, Korobelnik JF, Heier JS, et al. (2024). Intravitreal aflibercept 8mg in neovascular age-related macular degeneration (PULSAR): 48-week results from a randomised, double-masked, non-inferiority, phase 3 trial. *Lancet* 403:1141–52. doi: [10.1016/S0140-6736\(24\)00063-1](https://doi.org/10.1016/S0140-6736(24)00063-1).
- Leclercq B, Mejlachowicz D, Behar-Cohen F. (2022). Ocular barriers and their influence on gene therapy products delivery. *Pharmaceutics* 14:998. doi: [10.3390/pharmaceutics14050998](https://doi.org/10.3390/pharmaceutics14050998).
- Lin KH, Tran T, Kim S, et al. (2021). Advanced retinal imaging and ocular parameters of the rhesus macaque eye. *Transl Vis Sci Technol* 10:7. doi: [10.1167/tvst.10.6.7](https://doi.org/10.1167/tvst.10.6.7).
- Lin KH, Tran T, Kim S, et al. (2021). Age-related changes in the rhesus macaque eye. *Exp Eye Res* 212:108754. doi: [10.1016/j.exer.2021.108754](https://doi.org/10.1016/j.exer.2021.108754).
- Liu W, Borrell MA, Venerus DC, et al. (2019). Characterization of biodegradable microsphere-hydrogel ocular drug delivery system for controlled and extended release of ranibizumab. *Transl Vis Sci Technol* 8:12. doi: [10.1167/tvst.8.1.12](https://doi.org/10.1167/tvst.8.1.12).
- Liu W, Lee BS, Mieler WF, Kang-Mieler JJ. (2019). Biodegradable microsphere-hydrogel ocular drug delivery system for controlled and extended release of bioactive aflibercept in vitro. *Curr Eye Res* 44:264–74. doi: [10.1080/02713683.2018.1533983](https://doi.org/10.1080/02713683.2018.1533983).
- Liu W, Tawakol AP, Rudeen KM, et al. (2020). Treatment efficacy and biocompatibility of a biodegradable aflibercept-loaded microsphere-hydrogel drug delivery system. *Transl Vis Sci Technol* 9:13. doi: [10.1167/tvst.9.11.13](https://doi.org/10.1167/tvst.9.11.13).
- Luo L-J, Jian H-J, Harroun SG, et al. (2021). Targeting nanocomposites with anti-oxidative/inflammatory/angiogenic activities for synergistically alleviating macular degeneration. *Appl Mater Today* 24:101156. doi: [10.1016/j.apmt.2021.101156](https://doi.org/10.1016/j.apmt.2021.101156).
- Luo LJ, Nguyen DD, Lai JY. (2020). Benzoic acid derivative-modified chitosan-g-poly(N-isopropylacrylamide): Methoxylation effects and pharmacological treatments of Glaucoma-related neurodegeneration. *J Control Release* 317:246–58. doi: [10.1016/j.jconrel.2019.11.038](https://doi.org/10.1016/j.jconrel.2019.11.038).
- Lütjen-Drecoll E, Kaufman PL, Wasielewski R, et al. (2010). Morphology and accommodative function of the vitreous zonule in human and monkey eyes. *Invest Ophthalmol Vis Sci* 51:1554–64. doi: [10.1167/iov.09-4008](https://doi.org/10.1167/iov.09-4008).
- Mitchell JF, Boisvert CJ, Reuter JD, et al. (2014). Correction of refractive errors in rhesus macaques (*Macaca mulatta*) involved in visual research. *Comp Med* 64:300–8.
- Moshiri A, Chen R, Kim S, et al. (2019). A nonhuman primate model of inherited retinal disease. *J Clin Invest* 129:863–74. doi: [10.1172/JCI123980](https://doi.org/10.1172/JCI123980).
- Mozayan A, Farah S. (2013). Acute anterior uveitis following intravitreal injection of bevacizumab. *Ophthalmic Surg Lasers Imaging Retina* 44:25–7. doi: [10.3928/23258160-20121221-08](https://doi.org/10.3928/23258160-20121221-08).
- Nguyen DD, Luo LJ, Lai JY. (2019). Dendritic effects of injectable biodegradable thermogels on pharmacotherapy of inflammatory

- glaucoma-associated degradation of extracellular matrix. *Adv Health Mater* 8:e1900702. doi: [10.1002/adhm.201900702](https://doi.org/10.1002/adhm.201900702).
- Nguyen DD, Luo L-J, Lai J-Y. JY. (2020). Effects of shell thickness of hollow poly(lactic acid) nanoparticles on sustained drug delivery for pharmacological treatment of glaucoma. *Acta Biomater* 111:302–15. doi: [10.1016/j.actbio.2020.04.055](https://doi.org/10.1016/j.actbio.2020.04.055).
- Nguyen DD, Luo LJ, Yang CJ, Lai JY. (2023). Highly retina-permeating and long-acting resveratrol/metformin nanotherapeutics for enhanced treatment of macular degeneration. *ACS Nano* 17:168–83. doi: [10.1021/acsnano.2c05824](https://doi.org/10.1021/acsnano.2c05824).
- Orozco-Hernández A, Ortega-Larrocea X, Sánchez-Bermúdez G, et al. (2014). Acute sterile endophthalmitis following intravitreal bevacizumab: case series. *Clin Ophthalmol* 8:1793–9. doi: [10.2147/OPTH.S66230](https://doi.org/10.2147/OPTH.S66230).
- Osswald CR, Guthrie MJ, Avila A, et al. (2017). In vivo efficacy of an injectable microsphere-hydrogel ocular drug delivery system. *Curr Eye Res* 42:1293–301. doi: [10.1080/02713683.2017.1302590](https://doi.org/10.1080/02713683.2017.1302590).
- Osswald CR, Kang-Mieler JJ. (2015). Controlled and extended release of a model protein from a microsphere-hydrogel drug delivery system. *Ann Biomed Eng* 43:2609–17. doi: [10.1007/s10439-015-1314-7](https://doi.org/10.1007/s10439-015-1314-7).
- Osswald CR, Kang-Mieler JJ. (2016). Controlled and extended in vitro release of bioactive anti-vascular endothelial growth factors from a microsphere-hydrogel drug delivery system. *Curr Eye Res* 41:1216–22. doi: [10.3109/02713683.2015.1101140](https://doi.org/10.3109/02713683.2015.1101140).
- Park CY, Lee JK, Chuck RS. (2018). Toxic anterior segment syndrome—an updated review. *BMC Ophthalmol* 18:276. doi: [10.1186/s12886-018-0939-3](https://doi.org/10.1186/s12886-018-0939-3).
- Park MH, Jun HS, Jeon JW, et al. (2018). Preparation and characterization of bee venom-loaded PLGA particles for sustained release. *Pharm Dev Technol* 23:857–64. doi: [10.1080/10837450.2016.1264415](https://doi.org/10.1080/10837450.2016.1264415).
- Patel D, Patel SN, Chaudhary V, Garg SJ. (2022). Complications of intravitreal injections: 2022. *Curr Opin Ophthalmol* 33:137–46. doi: [10.1097/ICU.0000000000000850](https://doi.org/10.1097/ICU.0000000000000850).
- Rong X, Yuan W, Lu Y, Mo X. (2014). Safety evaluation of poly(lactic-co-glycolic acid)/poly(lactic-acid) microspheres through intravitreal injection in rabbits. *Int J Nanomed* 9:3057–68. doi: [10.2147/IJN.S64100](https://doi.org/10.2147/IJN.S64100).
- Rosenfeld PJ, Brown DM, Heier JS, et al. (2006). Ranibizumab for neovascular age-related macular degeneration. *N Engl J Med* 355:1419–31. doi: [10.1056/NEJMoa054481](https://doi.org/10.1056/NEJMoa054481).
- Rudeen KM, Liu W, Mieler WF, Kang-Mieler JJ. (2022). Simultaneous release of aflibercept and dexamethasone from an ocular drug delivery system. *Curr Eye Res* 47:1034–42. doi: [10.1080/02713683.2022.2053166](https://doi.org/10.1080/02713683.2022.2053166).
- Sato T, Emi K, Ikeda T, et al. (2010). Severe intraocular inflammation after intravitreal injection of bevacizumab. *Ophthalmology* 117:512–6.e2–516 e1–2. doi: [10.1016/j.ophtha.2009.07.041](https://doi.org/10.1016/j.ophtha.2009.07.041).
- Sazhnyev Y, Sin TN, Ma A, et al. (2023). Choroidal changes in rhesus macaques in aging and age-related drusen. *Invest Ophthalmol Vis Sci* 64:44. doi: [10.1167/iovs.64.12.44](https://doi.org/10.1167/iovs.64.12.44).
- Sengupta S, Chang DF, Gandhi R, et al. (2011). Incidence and long-term outcomes of toxic anterior segment syndrome at Aravind Eye Hospital. *J Cataract Refract Surg* 37:1673–8. doi: [10.1016/j.jcrs.2011.03.053](https://doi.org/10.1016/j.jcrs.2011.03.053).
- Stahl A. (2020). The diagnosis and treatment of age-related macular degeneration. *Dtsch Arztebl Int* 117:513–20. doi: [10.3238/arztebl.2020.0513](https://doi.org/10.3238/arztebl.2020.0513).
- Thackaberry EA, Farman C, Zhong F, et al. (2017). Evaluation of the toxicity of intravitreally injected PLGA microspheres and rods in monkeys and rabbits: effects of depot size on inflammatory response. *Invest Ophthalmol Vis Sci* 58:4274–85. doi: [10.1167/iovs.16-21334](https://doi.org/10.1167/iovs.16-21334).
- Turturro SB, Guthrie MJ, Appel AA, et al. (2011). The effects of cross-linked thermo-responsive PNIPAAm-based hydrogel injection on retinal function. *Biomaterials* 32:3620–6. doi: [10.1016/j.biomaterials.2011.01.058](https://doi.org/10.1016/j.biomaterials.2011.01.058).
- Wang F, Yu S, Liu K, et al. (2013). Acute intraocular inflammation caused by endotoxin after intravitreal injection of counterfeit bevacizumab in Shanghai, China. *Ophthalmology* 120:355–61. doi: [10.1016/j.ophtha.2012.07.083](https://doi.org/10.1016/j.ophtha.2012.07.083).
- Wickremasinghe SS, Michalova K, Gilhotra J, et al. (2008). Acute intraocular inflammation after intravitreal injections of bevacizumab for treatment of neovascular age-related macular degeneration. *Ophthalmology* 115:1911–5. doi: [10.1016/j.ophtha.2008.05.007](https://doi.org/10.1016/j.ophtha.2008.05.007).
- Wykoff CC, Brown DM, Reed K, et al. (2023). Effect of high-dose intravitreal aflibercept, 8 mg, in patients with neovascular age-related macular degeneration: the phase 2 CANDELA randomized clinical trial. *JAMA Ophthalmol* 141:834–42. doi: [10.1001/jamaophthalmol.2023.2421](https://doi.org/10.1001/jamaophthalmol.2023.2421).
- Xu L, Lu T, Tuomi L, et al. (2013). Pharmacokinetics of ranibizumab in patients with neovascular age-related macular degeneration: a population approach. *Invest Ophthalmol Vis Sci* 54:1616–24. doi: [10.1167/iovs.12-10260](https://doi.org/10.1167/iovs.12-10260).
- Zhu Q, Ziemssen F, Henke-Fahle S, et al. (2008). Vitreous levels of bevacizumab and vascular endothelial growth factor-A in patients with choroidal neovascularization. *Ophthalmology* 115:1750–5, 1755 e1. doi: [10.1016/j.ophtha.2008.04.023](https://doi.org/10.1016/j.ophtha.2008.04.023).